Optoelectronic Applications of Hybrid Luminescent Nanocomposites

M.Sc. Thesis

By

KASHISH GUPTA

DEPARTMENT OF CHEMISTRY

INDIAN INSTITUTE OF TECHNOLOGY INDORE

MAY 2023

Optoelectronic Applications of Hybrid Luminescent Nanocomposites

A THESIS

*Submitted in partial fulfillment of the
requirements for the award of the degree*

of

Master of Science

by

KASHISH GUPTA

2103131009

DEPARTMENT OF CHEMISTRY

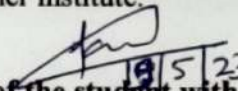**INDIAN INSTITUTE OF TECHNOLOGY**

INDORE

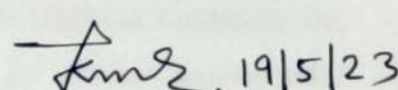**MAY 2023**

INDIAN INSTITUTE OF TECHNOLOGY INDORE

CANDIDATE'S DECLARATION

I hereby certify that the work which is being presented in the thesis entitled **"Optoelectronic Applications of Hybrid Luminescent Nanocomposites"** in the partial fulfillment of the requirements for the award of the degree of **MASTER OF SCIENCE** and submitted in the **DEPARTMENT OF CHEMISTRY, Indian Institute of Technology Indore**, is an authentic record of my own work carried out during the time period from June, 2022 to May, 2023 under the supervision of **Prof. Tushar Kanti Mukherjee**, Professor, IIT Indore.
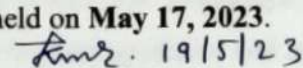
The matter presented in this thesis has not been submitted by me for the award of any other degree of this or any other institute.
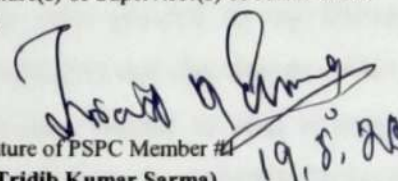
Signature of the student with date
KASHISH GUPTA

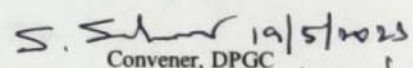---

This is to certify that the above statement made by the candidate is correct to the best of our knowledge.
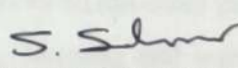
Signature of Thesis Supervisor with date
Prof. TUSHAR KANTI MUKHERJEE

KASHISH GUPTA has successfully given his M.Sc. Oral Examination held on **May 17, 2023**.

Signature(s) of Supervisor(s) of M.Sc. thesis
Date:

Convener, DPGC
(Dr. Umesh A. Kshirsagar)
Date:

(Dr. Selvakumar
Acting DPAC

Signature of PSPC Member #1
(Dr. Tridib Kumar Sarma)
Date

Signature of PSPC Member #2
(Dr. Selvakumar Sermadurai)
Date: 19/5/2023

ACKNOWLEDGEMENTS

Dedicated to My family

and All Friends

x

ABSTRACT

In modern time, nanoparticles have been utilized extensively as a photocatalyst for removing a wide range of contaminants from polluted water such as organic dyes, pesticides, pharmaceutical waste etc. Herein, we have utilized a new type of inorganic-organic hybrid coacervates as photocatalytic nanoreactor. We fabricated a new CD-embedded hybrid coacervate by simple mixing of anionic carbon dots (CDs) and cationic polymer poly (diallyl dimethylammonium chloride) (PDADMAC) and equilibrated this binary mixture for 12 h at room temperature to get CD-embedded droplets (CD-Ds) via electrostatic interactions. Next, these CD-Ds were utilized for the selective detection of pharmaceutical contaminants in waste water. Here we have found that the photoluminescence (PL) intensity of these droplets was quenched specifically in the presence of TCH and DXH only while little to no change was observed in presence of other pharmaceutical waste. Furthermore, after the detection of TCH and DXH, we explored the role of CD-Ds towards photocatalytic degradation of pharmaceuticals. Interestingly, CD-Ds were found to sequester TCH and DXH upon incubation for 4 h with a partition coefficient of 9.4 ± 0.2 and 7.9 ± 0.1, respectively. Notably, we observed a significant enhancement in the photocatalytic degradation of TCH and DXH in presence of TCH/DXH-loaded CD-Ds as compared to bare CDs under the illumination of blue light. The mechanistic studies in the presence of various radical scavengers shows that superoxide radicals and holes are mainly responsible for the photocatalytic degradation of TCH and DXH. Our present CD-Ds system was found to exhibit good recyclability toward photocatalytic degradation of TCH for five consecutive runs under blue light illumination. Therefore, our present CD-Ds system is easy to fabricate and applicable for the detection as well as visible light driven photocatalytic degradation of TCH and DXH.

TABLE OF CONTENTS

Chapter 1: Introduction

1.1.   Nanoscience and Nanotechnology

1.2.   Nanoparticles

      1.2.1.   Quantum Dot

      1.2.1.1. CdTe Quantum Dot

      1.2.2.   Carbon Dot

1.3.   Coacervates

1.4.   Environmental Contaminants

      1.4.1.   Pharmaceutical Contaminants

Chapter 2: Experimental Section

2.1.   Chemicals

2.2.   Synthetic Procedures

      2.2.1. Synthesis of MSA Ligand-Capped CdTe QDs

      2.2.2. Synthesis of Carbon Dots

2.3.   Fabrication of Droplets

      2.3.1. Fabrication of QD-Ds

      2.3.2. Fabrication of CD-Ds

2.4.   Partitioning of TCH and DXH in CD-Ds

2.5.   Instrumentation

LIST OF SCHEMES

Scheme 1. Schematic representation of top-down and bottom-up approaches.

Scheme 2. Schematic representation of synthesis of CdTe QDs.

Scheme 3. Schematic illustration of synthesis of CD and CD-Ds.

Scheme 4. Schematic illustration of CD-Ds in the presence of TCH and DXH.

LIST OF FIGURES

Figure 1. Different types of NPs.

Figure 2. Various applications of NPs.

Figure 3. Representation of exciton when photon is absorbed by quantum dot (QD).

Figure 4. Demonstration of some applications of QDs.

Figure 5. Photograph of green and red emissive CdTe QDs under UV light illumination.

Figure 6. Confocal images of (A) blue emissive, (B) green emissive, and (C) red emissive coacervate droplets.

Figure 7. Various sources of environmental contaminants.

Figure 8. (A) Absorption and emission spectra of CDs. (B) TEM image of CDs. (C) FTIR spectra of CDs. (D) Representation of formation of CD-Ds. (E) Confocal images (DIC, fluorescence) of CD-Ds.

Figure 9. (A) Changes in PL intensity of CD-Ds in the presence of 50 and 100 μM of both TCH and DXH. (B) PL responses of the system CD-Ds towards other pharmaceuticals. (C) Anti-interference ability and selectivity of CD-Ds towards TCH and DXH sensing in the presence of other pharmaceuticals (1.0 equivalent). (D) Photograph of CD-Ds solutions in the presence and absence of several pharmaceuticals (100 μM) under UV light illumination.

Figure 10. Stern Volmer plots of CD-Ds with TCH and DXH, respectively, concentrations (1-50 μM) in the presence of (A, B) Milli-Q and (C, D) tap water.

Figure 11. Confocal images (DIC, fluorescence) in the absence and presence of TCH and DXH.

Figure 12. PL decay curves in the absence and presence of TCH and DXH of (A) CDs and (B) CD-Ds. UV spectra of Only CD-Ds and (C) TCH or (D) DXH.

Figure 13. C_t/C_o plots of (A) TCH and (C) DXH at different conditions under blue light illumination for 75 min. The first order kinetics plots of -$\ln(C_t/C_o)$ *vs* time for (B) TCH and (D) DXH at different conditions under blue light illumination for 75 min.

Figure 14. (A) % Degradation of TCH with CD-Ds in the presence of various radical scavengers. (B) Recyclability experiment of CD-Ds for photocatalytic degradation of TCH under blue light illumination for five consecutive runs. Confocal images (DIC) of droplets (C) before first cycle (D) after fifth cycle.

Figure 15. Possible mechanism of photocatalytic degradation of TCH and DXH.

ABBREVIATIONS

CDs	Carbon dots
CD-Ds	Carbon Dot-Droplets
CdTe	Cadmium Tellurium
CLSM	Confocal laser scanning microscopy
DIC	Differential interference contrast
DXH	Doxycycline hyclate
FESEM	Field emission scanning electron microscopy
FTIR	Fourier transform infrared spectroscopy
IFE	Inner filter effect
IRF	Instrument response function
LOD	Limit of detection
LLPS	Liquid-liquid phase separation
MSA	Mercaptosuccinic acid
NDs	Nanodroplets
NPs	Nanoparticles
PDADMAC	poly diallyldimethylammonium chloride
PL	Photoluminescence
QDs	Quantum dots
TCH	Tetracycline hydrochloride
TCSPC	Time-correlated single-photon counting
TEM	Transmission electron microscopy
UV	Ultraviolet
Vis	Visible

NOMENCLATURE

cm	Centimeter
°C	Degree Celcius
g	Gram
h	Hour
m	Meter
μL	Microliter
μm	Micrometer
μM	Micromolar
mg	Milligram
mL	Milliliter
mm	Millimeter
mM	Millimolar
min	Minute
M	Molar
nm	Nanometer
nM	Nanomolar
ns	Nanoseconds
%	Percentage
Rpm	Revolution per minute
λ_{em}	Emission wavelength
λ_{ex}	Excitation wavelength
pH	The negative logarithm of hydronium-ion concentration

Chapter 1: INTRODUCTION

1.1. Nanoscience and Nanotechnology

Nanoscience is the science in which structures and matters possess its size at nanoscale and it can be utilized for various practical applications, called nanotechnology.[1] The electronic and optical properties of nanomaterials are different from their larger counterpart. The field of nanoscience and nanotechnology are progressing rapidly every year in various research area. In the 21st century, nano things are not new and many researchers have been working with polymers and some small sub-units since many decades. This word 'nano' is taken from the Greek word 'dwarf' whose meaning is 'very small thing or object'.[2] It represents one billionth of a meter i.e., one nanometer (nm) is equal to 10^{-9} meter (m).

Scheme 1. Schematic Representation of Top-Down and Bottom-Up Approaches.
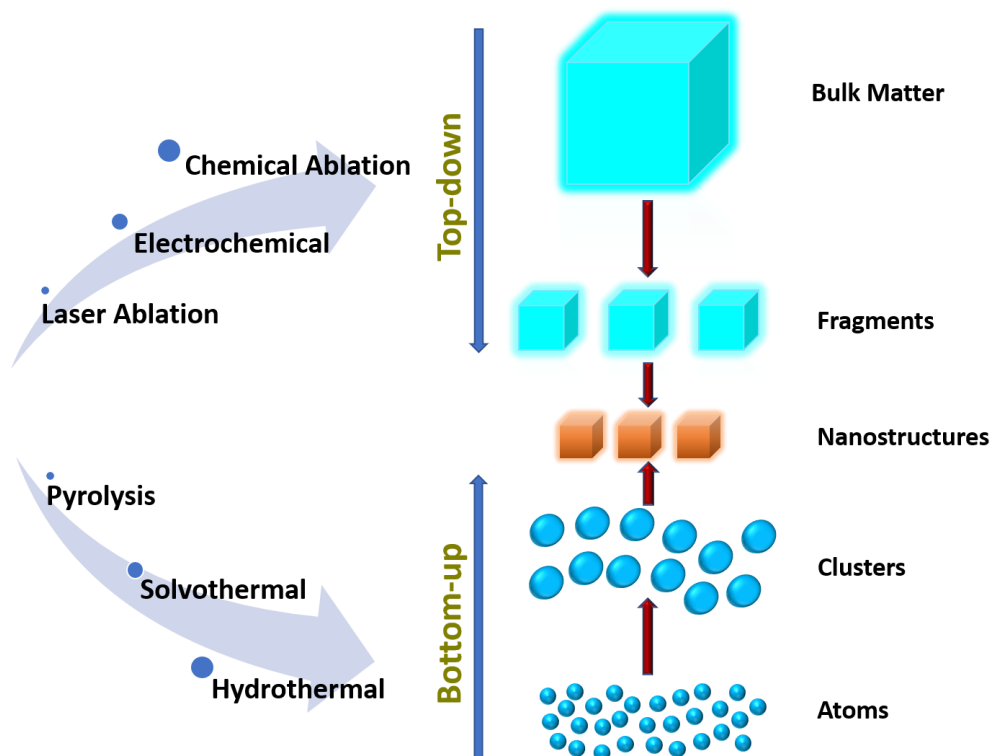
At first, Richard Feynman, the american physicist and the nobel prize winner, explained the phenomena of nanotechnology in 1959.[2] He is also

considered the father of nanotechnology. Furthermore, a japanese scientist Norio Taniguchi called the term 'nanotechnology' and defined very well in 1974.[1]

The synthesis of various nanomaterials/nanostructures mainly follow two approaches i.e., top-down and bottom-up approach. When bulk materials are broken down into smaller NPs it is called top-down method while when nanostructures are synthesized by using different small atoms, metal salts, or molecules it is known as bottom-up method.[2] Nanomaterials are utilized in various applications[3-8] like fuel cells, batteries, paints, displays, catalysts and making sunscreens, cosmetics, composites, clays, coatings or surfaces and for long term use; carbon nanotube composites, lubricants, medical implants, magnetic materials, military battle suits etc.

1.2. Nanoparticles

NPs or Ultrafine particles are quite small in size in any material which lie within the size range of 1 to 100 nm.[9] They are undetected to the human eye and exhibits different physical or chemical properties like; colloidal properties, electric properties, mechanical properties due to their smaller size. Most of the NPs are made by few hundred atoms. There are several categories of NPs like;

(1) Carbon-based NPs   (2) Organic-based NPs

(3) Inorganic-based NPs   (4) Composite-based NPs
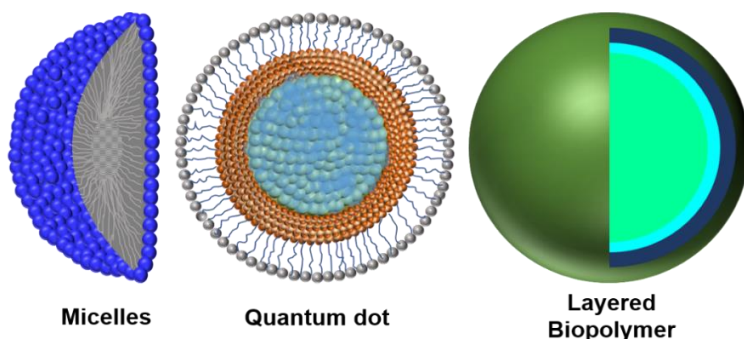
Figure 1. Different types of NPs.

There are variety of applications in which NPs play important role like; biomedical, photocatalysis, nanoreactors, biosensing etc. Based on their compositions, NPs have three categories; Organic, Carbon-based and Inorganic.
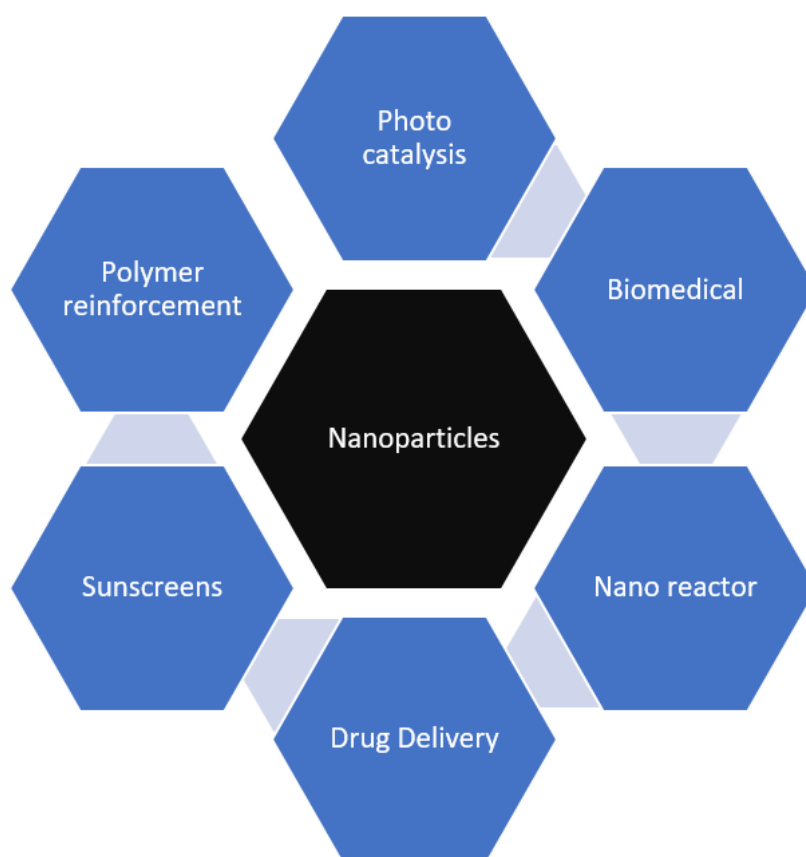
Figure 2. Various applications of NPs.

1.2.1. Quantum Dot

In 1981, Russian Physicist Alexey Ekimov was the first person who observed Quantum Dots (QDs) in a glass matrix.[10] These dots are quite small in size and show quantum confinement effect thus they are called QDs.[11] Furthermore, they are also referred as artificial atoms.[12] QDs are semiconducting nanocrystals having unique electronic, optical and photophysical properties. They are few nm in size ranging from 2 to 10

nm. As usual, 1 nm is equal to 10^{-9} m. They emit a particular color upon illumination by UV light which mainly depends on the size of QDs i.e., they show size dependent emission properties.

As we know, when an electron excites from its lower energy level to higher energy level that means electron leaves its valence band and excites to the conduction band. Subsequently, after returning back to the valence band of that electron, it liberates its energy in the form of light. The particular color of liberating light, depends on the energy difference between the valence band and the conduction band of QDs.
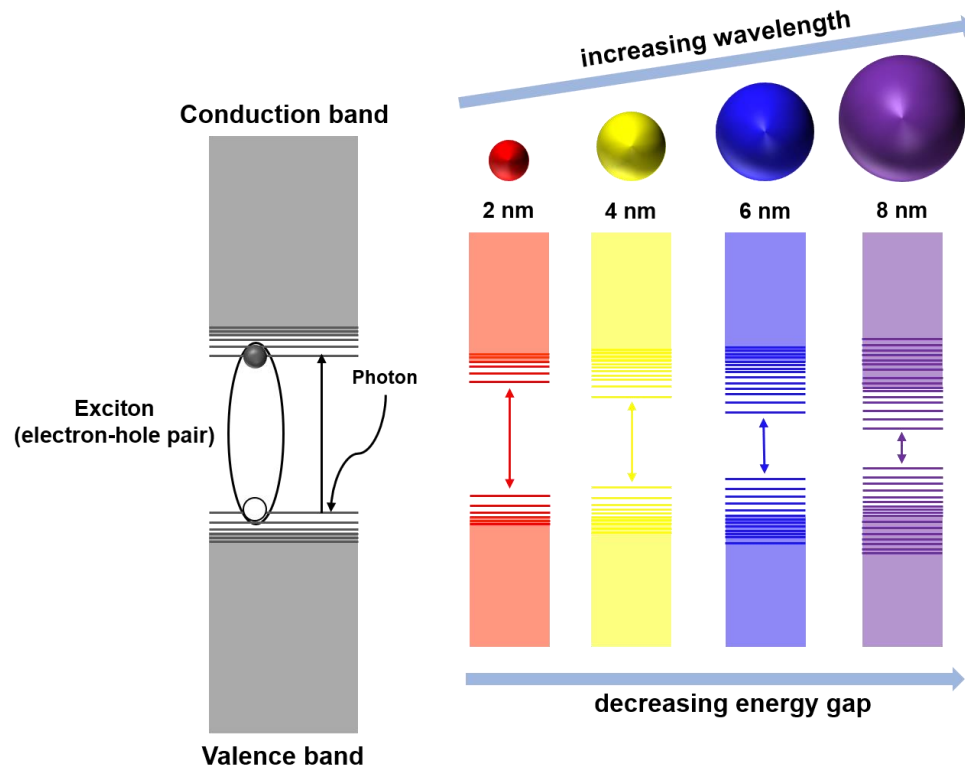
Figure 3. Representation of exciton when photon is absorbed by QD.

Shorter wavelengths have found in smaller QDs (2-3 nm) and they exhibit the color spectrum from violet to green. Longer wavelengths have seen by larger QDs (5-6 nm) with the color spectrum from yellow to red.

Therefore, their optoelectronic properties and the specific color vary, depending on both size and shape of QDs.[13]

There are so many optical applications of QDs due to its high photostability and high molar extinction coefficients. QDs are used in bioimaging, photovoltaic devices[14], light emitting devices[15], photocatalyst and photodetector devices[16] etc.
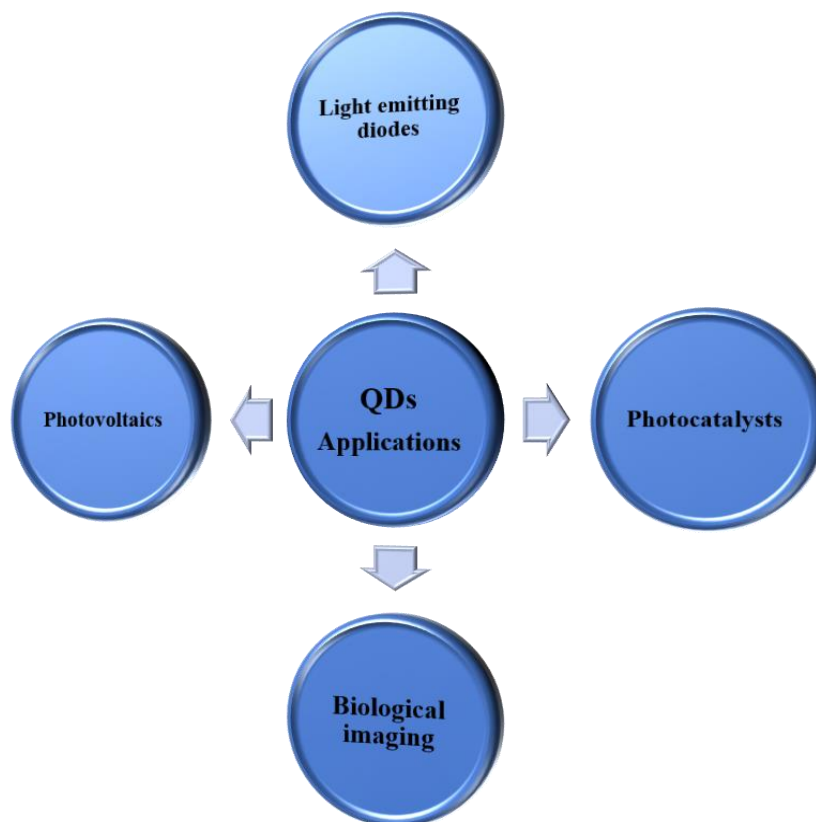
Figure 4. Demonstration of some applications of QDs.

1.2.1.1. CdTe Quantum Dot

CdTe (Cadmium Tellurium) QDs are one of the many examples of QDs which have various applications due to its small band gap energy (1.44 eV) and larger exciton Bohr radius (almost 6.5 nm).[17] They are highly stable and water soluble and having high quantum yield of (20-90 %), synthesized via colloidal chemical route. There are also many methods to prepare CdTe QDs.
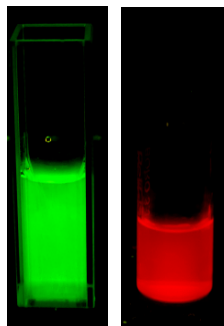
Figure 5. Photograph of green and red emissive CdTe QDs under UV light illumination.

1.2.2. Carbon Dot

CDs are quasi-zero-dimensional carbon-based materials in the size range of 2-20 nm.[18] CDs have emerged as the rising star in nanotechnology because of its magical properties like high quantum yield, low venomousness, small size, good biocompatibility, tunable photoluminescence (PL) and low-cost sources. They show strong absorption in the UV region (200-400 nm) with a tail going to the visible range.

At first, carbon NPs were accidently obtained as a byproduct during the purification of single-walled carbon nanotubes. Yang's group synthesized polymer-like CDs from citric acid and ethylenediamine with quantum yield 81% via one-step hydrothermal method.[19] There are many applications of CDs in various fields like biomedicine, catalysis, optoelectronic devices, anti-counterfeiting[20-23] etc.

1.3. Coacervates

Coacervates are organic, aqueous phase, small, polymer-rich dense droplets. They are formed via liquid-liquid phase separation[24-27], resulting from association of two oppositely charged molecules[28,29] (polyelectrolytes, proteins) via electrostatic interaction. This kind of process leads to the fabrication of roughly circular, round coacervate

droplets within the size limit between a few nm to some micrometers (μm).

The word 'Coacervation' comes from Latin word "Coacervare" whose meaning is 'to assemble together or clusters'. This Coacervation process was proposed by Russian biochemist Aleksandar Oparin and British biologist J.B.S. Haldane in his theory.
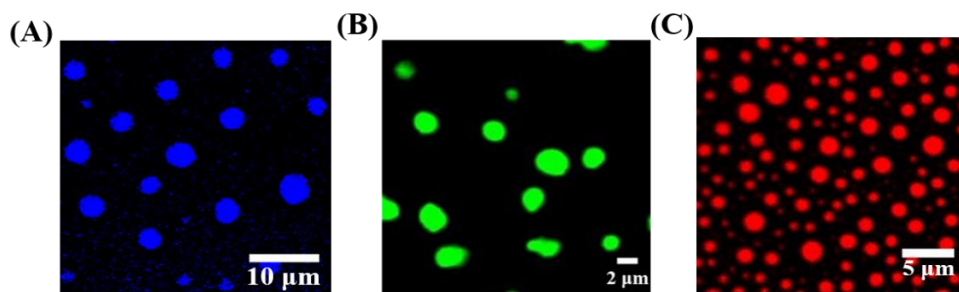
Figure 6. Confocal images of (A) blue emissive, (B) green emissive, and (C) red emissive coacervate droplets.

1.4. Environmental Contaminants

In modern time, as people want more and more facilities, its side-effects are increasing side-by- side and here comes environmental issues like; pharmaceuticals contaminants, heavy metal ions, waste disposal, agrochemicals, industries, pesticides, plastics, personal care products etc. Water bodies and human health are affecting by these environmental pollutions. This 'environment contaminant' term is mainly used to elaborate a condition of "no outer process of unwanted materials in its substantial form or energy form". It can be in the form of low concentration of any type of chemicals, in the form of waste in the water, in the air, soil and in our atmosphere. We will have to minimize these pollutants from our environment.
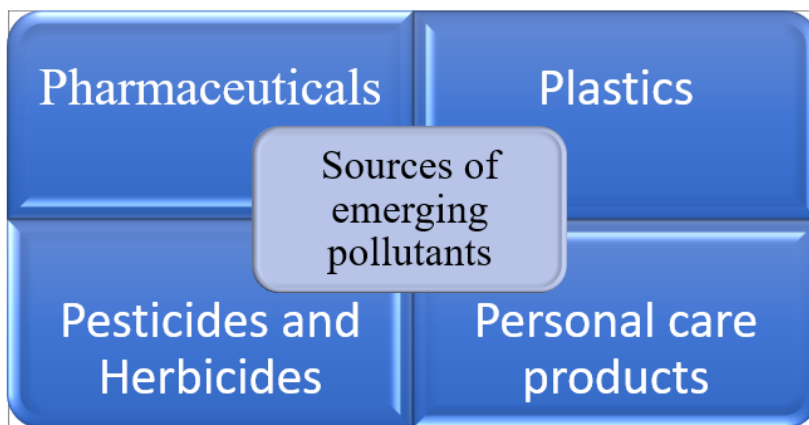
Figure 7. Various sources of environmental contaminants.

1.4.1. Pharmaceutical Contaminants

Among the various environmental contaminants, pharmaceutical contaminants are one of the major contaminants which pollutes the water bodies. A sharp increment has been shown in increasing of industries and its manufacturing products like lotion, toothpaste, shampoos, soaps, sunscreens, cosmetic over the past few decades. With the increasing demand of chemical products and pharmaceuticals; human health, ecosystem and water bodies are negatively influenced by the side-effects of these materials. Even though pharmaceuticals active substances are present in lower amount but they exist for long-time periods with their stable forms and structures.

Tetracyclines and Doxycycline are mainly used to control and prevent the micro-organic infections because of its anti-bacterial effect, lower cost and good availability. But long-time period uses and overdose of it, produces issues directly on human organs, livers, toxicity problem, allergic problems, etc.[30] Their presence also harms the aquatic life. They possess stable structures so they do not degrade easily. Therefore, there is a high necessity for design and fabrication of simple yet effective nanocomposites for their detection as well as removal from the contaminated water.

Chapter 2:   EXPERIMENTAL SECTION

2.1.   Chemicals

Trisodium citrate dihydrate ($Na_3C_6H_5O_7.2H_2O$), poly(diallyldimethylammonium chloride) (PDADMAC,   MW = 100000-200000), cadmium chloride ($CdCl_2$), sodium borohydride ($NaBH_4$), mercaptosuccinic acid (MSA), sodium tellurite (Na_2TeO_3), citric acid ($HOC(CO_2H)(CH_2CO_2H)_2$), ethylenediamine ($C_2H_4(NH_2)_2$), tetracycline hydrochloride ($C_{22}H_{25}ClN_2O_8$), doxycycline hyclate ($C_{24}H_{33}ClN_2O_{10}$), streptomycin sulphate ($C_{21}H_{41}N_7O_{16}S$), vancomycin hydrochloride ($C_{66}H_{76}Cl_3N_9O_{24}$), ampicillin sodium salt ($C_{16}H_{18}N_3NaO_4S$), amoxicillin trihydrate ($C_{16}H_{25}N_3O_8S$), ciprofloxacin hydrochloride ($C_{17}H_{19}ClFN_3O_3$), norfloxacin ($C_{16}H_{18}FN_3O_3$), ibuprofen ($C_{13}H_{18}O_2$), erythromycin ($C_{37}H_{67}NO_{13}$), dopamine hydrochloride ($C_8H_{11}NO_2$), D-glucose ($C_6H_{12}O_6$), t-butyl alcohol ($C_4H_{10}O$), benzoquinone ($C_6H_4O_2$), ethylenediaminetetraacetic acid disodium salt ($C_{10}H_{18}N_2Na_2O_{10}$), Pur-A-Lyzert dialysis kit (MW- cut-off 3.5kDa) bought from Sigma- Aldrich, Hellmanex III. MQ water, gained from a Millipore purifying machine (Milli-Q integral).

2.2.   Synthetic Procedures

We have synthesized CdTe QDs, CDs according to the previous reported procedure.

2.2.1.   Synthesis of MSA Ligand-Capped CdTe QDs

At first, we have taken 50 mL Milli-Q water in one necked round bottom flask by measuring cylinder. 29.32 mg cadmium chloride in 4 mL Milli-Q water was mixed into this flask and we have added trisodium citrate dihydrate (100 mg), sodium tellurite (2.2 mg/mL) and mercaptosuccinic acid (50 mg) simultaneously.

After this, we have added sodium borohydride (100 mg) and quick covered with silver foil. When the mixture turned to the green color, the flask was engaged to condenser and refluxed for 0.5 h under open-air condition to achieve green luminescent QDs. The mixture was decontaminated by dialysis membrane for 24 h in the Milli-Q water to detach impurities, unreacted reactants and dissociated MSA ligands. The purified CdTe QDs was kept in refrigerator at 4 °C for further works.[31,32]

Scheme 2. Schematic Representation of Formation of CdTe QDs.
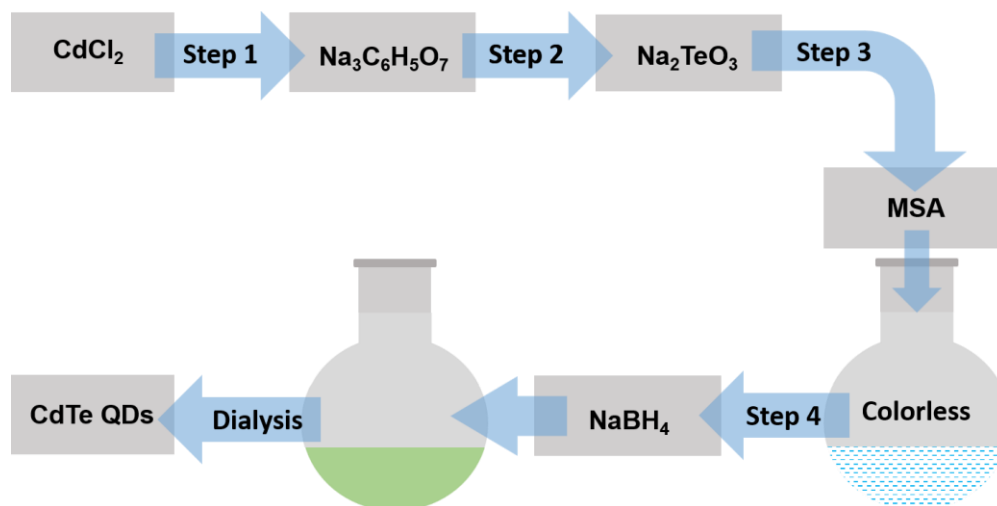
2.2.2. Synthesis of Carbon Dots

Firstly, citric acid (1.015 g) was diluted in 10 mL Milli-Q water via sonicating for 5 min. After this, 335 μL ethylenediamine was taken and added into it and sonicated again for 5 min to dissolve. Then the reaction mixture was taken into 25 mL Teflon-padded autoclave for giving it high pressure and temperature and heated at 200°C temperature for 5 h. After completion of time, the reactor was cooled at room temperature. The solution was kept for dialysis to remove impurities and excess unreacted starting materials from the mixture.[33,34]

2.3. Fabrication of Droplets

We have synthesized QD-Ds and CD-Ds via previously reported method.

2.3.1. Fabrication of QD-Ds

We have taken 300 μL QDs and 180 μL PDADMAC (2 μL polymer in 1 mL Milli-Q) in 3 mL Milli-Q water at the room temperature for the fabrication of droplets. This mixture was equilibrated for 4 h at room temperature to obtain well dispersed spherical stable droplets.[35] After this, sample was drop-casted on cleaned and washed coverslips and dried for imaging. Coverslips were cleanup by using Hellmanex and dilute chromic acid.

2.3.2. Fabrication of CD-Ds

At first, 0.06 mg/mL CDs were dissolved in pH 10 and then 32 μM PDADMAC was mixed at room temperature for the fabrication of CD-Ds.

Scheme 3. Schematic Illustration of Synthesis of CD and CD-Ds.
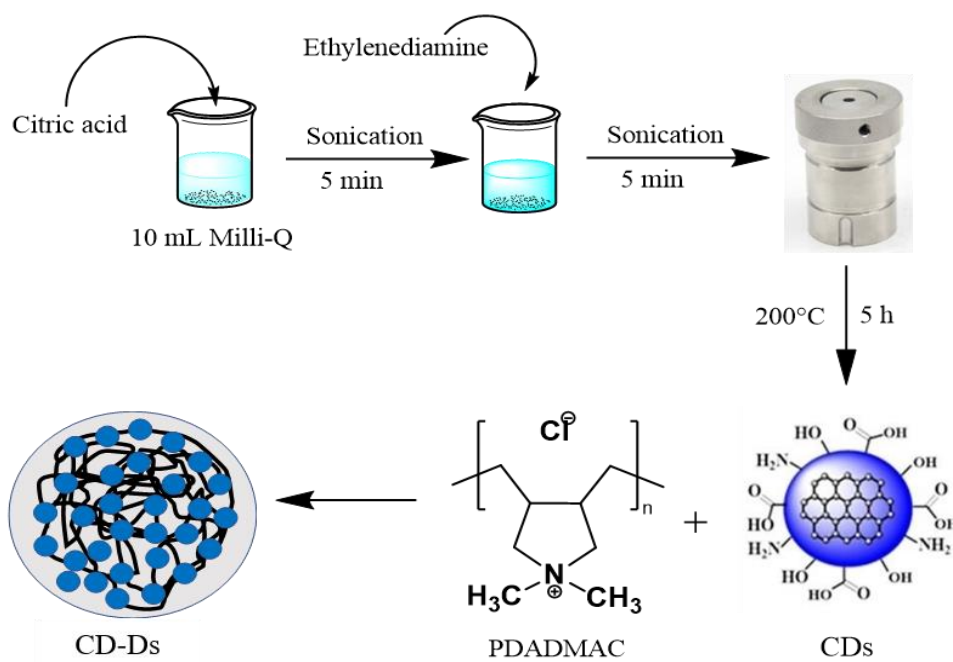
This binary mixture was equilibrated for 1 and 18 hours to get small droplets and large droplets. This pH 10 was made with 0.1 M NaOH.[36] Samples were drop-casted on properly washed and cleaned coverslips for microscopic experiments. Coverslips were washed by using Hellmanex and dilute chromic acid and dried for imaging.[32,37]

2.4. Partitioning of TCH and DXH in CD-Ds

At first, we synthesized 1 mM stock solution of TCH and DXH. After this, we mixed 100 μM TCH and DXH solution one by one into the CD-Ds. This reaction mixture was equilibrated for 4 h at room temperature. This reaction mixture was centrifuged at 20,000 rpm for 30 min to obtain TCH and DXH loaded CD-Ds. The emphatic concentration of encapsulated TCH and DXH in the CD-Ds and free TCH and DXH in the supernatant phase was calculated by using the UV-vis spectrophotometer. The partition coefficient (K) was calculated by the help of this equation:

$$K = \frac{[Substrate]_{CD-Ds}}{[Substrate]_{Supernatant}}$$

2.5. Instrumentation

We have studied different type of spectroscopic and microscopic techniques for the characterization of as-synthesized CDs and CD-Ds.

2.5.1. UV-vis Spectrophotometer

The normalized absorption spectra were measured in a 3.5 mL cuvette made by quartz (1×1 cm^2) by UV-vis spectrophotometer (Carry 100 Bio). The spectra were corrected by using solvent absorption as the baseline. UV-vis spectrophotometer is commonly used for the quantitative determination of the sample in the analytical chemistry like; water-soluble high conjugating organic compounds, transition metals, more intensive charge transfer complexes etc.

2.5.2. Spectrofluorometer

The PL spectra were measured in a 3.5 mL cuvette made by quartz (1×1 cm^2) with both excitation and emission slit width in size ranging from 1 to 5 nm with Fluoromax-4 Spectrofluorometer (HORIBA Jobin Yvon, model FM-100). This instrument provides the information of properties of fluorescent molecules at certain wavelength. This instrument works in the solution as well as solid state and no need to take baseline correction.

2.5.3.   Confocal Laser Scanning Microscopy (CLSM)

CLSM image was captured to see the shape, morphology and structure of CD-Ds by using confocal microscopy (Olympus, model number FV1200MPE, IX-83) and samples were excited by diode lasers (559, 488 and 405 nm). For all kind of microscopy measurements, we have washed coverslips with Hellmanex and dilute chromic acid and dried for imaging. We have drop-casted our samples on cleaned and dried coverslips and dried overnight in the desiccator.

2.5.4.   Field Emission Scanning Electron Microscopy (FE-SEM)

FE-SEM images of CD-Ds were obtained by using instrumentation of Supra 55 Zeiss FE-SEM. This microscopic technique is just like confocal microscopic technique but in high resolution as compared to confocal imaging technique. SEM images have large resolution than confocal images. For this microscopy technique, we drop-casted our samples on properly washed and cleaned glass-slides.

2.5.5. Transmission Electron Microscopy (TEM)

TEM images of CDs were captured by using TECNAI G2 200 kV TEM (FEI, Electron Optics) with 200 kV input voltage equipped with a LaB6 source. This microscopic technique tells the information of size and morphology of CDs. This imaging technique is also like confocal imaging technique but measures the size of sample in nm range as compared to μm range in confocal microscopy i.e., TEM images are highly magnified images.

2.5.6. Fourier Transform Infrared Spectroscopy (FTIR)

FTIR spectra was measured by using Tensor-27 Bruker spectrometer in a KBr pellet of CDs on which some functional groups are attached on the surface of CDs. This spectroscopic technique is used to provide the information about chemical composition and basic profile of the whole sample. FTIR technique detects the functional groups of the sample like; −NH, −CH, −OH, −COOH, −CN etc. KBr is used as a carrier in the form of pellet or disk.

2.5.7. Time-Correlated Single-Photon Counting (TCSPC)

TCSPC technique is useful for the measuring the fluorescence decay or fluorescence lifetime in time domains. The principle of the TCSPC technique is that it detects the single photons and measures arrival times of them with respect to light source, a reference signal. A picosecond diode laser (model Pico Brite-375L and DD-450L) was used to excite the samples with excitation wavelength of 405 nm.

Chapter 3: RESULTS AND DISCUSSION

3.1. Synthesis and Characterization of CDs and CD-Ds

The blue emissive CDs were synthesized according to previously reported method[33,34] and were characterized using different spectroscopic and microscopic techniques. This as-synthesized CDs show the normalized absorption peak at 340 nm due to the n-π^* transition from the C=O functional group attached on the surface of CDs and weak shoulder near 250 nm displays due to the π-π^* transition of aromatic sp^2 carbon (Figure 8A). The CDs show a prominent PL maximum at 442 nm upon the excitation at 340 nm.
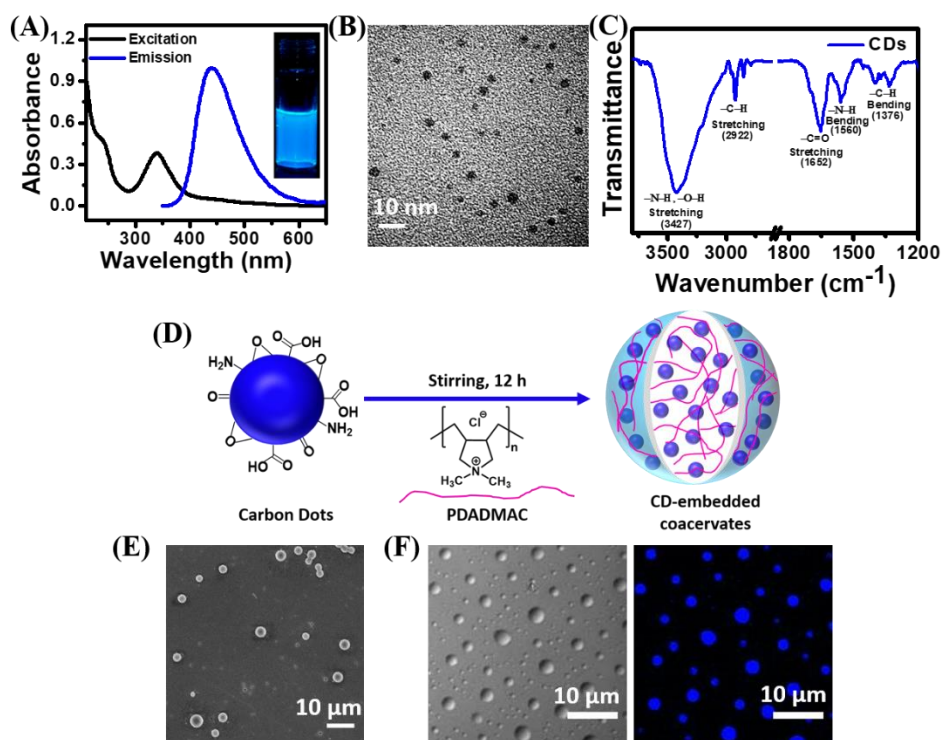
Figure 8. (A) Absorption and emission spectra, (B) TEM image, and (C) FTIR spectra of CDs. (D) Schematic representation of fabrication of CD-Ds. (E) FESEM image and (F) Confocal images (DIC, fluorescence) of CD-Ds.

Furthermore, they show intense blue color in the aqueous solution upon illumination under UV light of 365 nm (Figure 8A, inset).

The present CDs show excitation independent emission in the excitation range of 300-390 nm. Furthermore, these CDs were found to be highly stable upon storing for multiple days with no change in its absorption of emission behavior.[33,38] Figure 8B shows the TEM image of CDs that shows multiple spherical dots and uniform size of CDs. Notably, the mean size of CDs was estimated to be $2.9 \pm 0.1$ nm. Our findings clearly reveal the successful synthesis of blue emissive CDs with a uniform size range. We further recorded the FTIR spectra of CDs to know about the functional groups attached on the surface of CDs as shown in Figure 8C. The peak near 3427 cm^{-1} attributes to the stretching vibrations of N−H and O−H moieties. The two peaks near at 1560 and 1652 cm^{-1} are due to the presence of bending and stretching vibrations of N−H and C=O functional groups, respectively while the other two peaks present near at 1376 and 2922 cm^{-1} are due to the bending and stretching vibrations of C−H moiety, respectively. Our findings reveal the presence of different functional groups like −NH_2, −OH and −COOH over the surface of CDs.

The CD-Ds were fabricated via electrostatic interaction by simply mixing of cationic polymer poly(diallyl dimethylammonium chloride) (PDADMAC) and anionic CDs using previously reported method (Figure 8D). This binary solution was equilibrated for 12 h with constant stirring at room temperature to obtain the uniform CD-Ds. Figure 8E shows FE-SEM image which confirms the presence of well dispersed stable spherical droplets present in this binary mixture. We further explored the luminescent properties of CD-Ds using CLSM (Figure 8F). We drop-casted our samples of CD-Ds on properly washed and cleaned coverslips and captured the confocal images of CD-Ds after excitation with 405 nm diode laser. The differential interference contrast (DIC) image of CD-Ds confirms the presence of uniformly dispersed stable droplets inside the

binary solution. Interestingly, the blue emission manifests specifically from inside of these droplets which confirms the presence of CDs inside these self-assembled droplets.

3.2. Sensing of Pharmaceuticals with CD Droplets

The Figure 9A shows the PL spectra of CD-Ds in the presence of different concentrations of tetracycline (TCH) and doxycycline (DXH). The PL intensity of droplets, decreases in the presence of 50 and 100 μM concentrations of TCH and DXH. It is clearly evident that the PL intensity of CD-Ds, decreases almost 2.2fold and 4.7fold in the presence of 50 and 100 μM concentrations of both TCH and DXH, respectively. Next, we explored selectivity of CD-Ds towards different pharmaceuticals (Figure 9B). Notably, no appreciable change was observed in the I/I_0 values of CD-Ds in the presence of other pharmaceuticals while only in the presence of 100 μM TCH and DXH, a prominent change was observed in the I/I_0 values of CD-Ds.
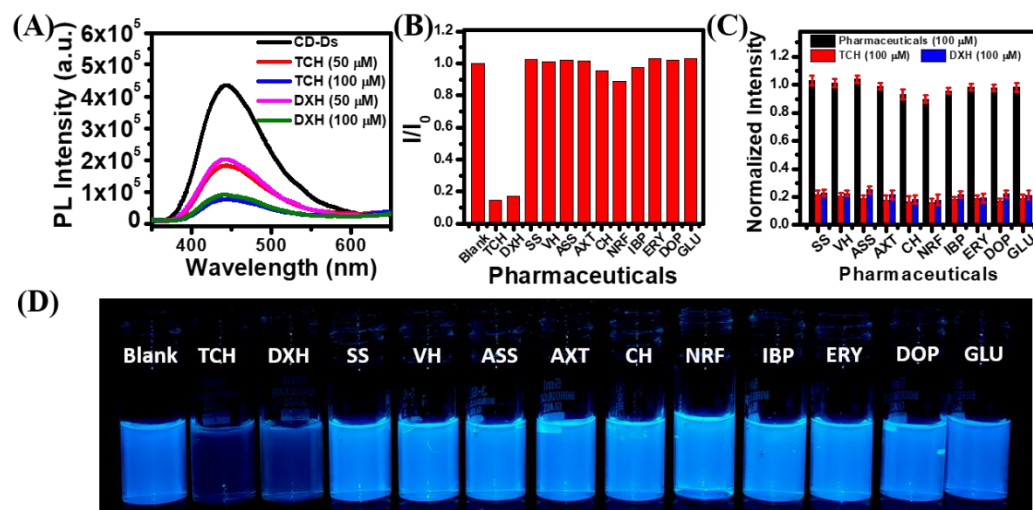
Figure 9. (A) Changes in PL intensity of CD-Ds in the presence of 50 and 100 μM of both TCH and DXH. (B) PL responses of our system CD-Ds towards other pharmaceuticals. (C) Anti-interference ability and selectivity of CD-Ds towards TCH and DXH (1.0 equivalent) sensing in the presence of other pharmaceuticals (1.0 equivalent). (D) Photograph of

CD-Ds solutions in the presence and absence of several pharmaceuticals (100 μM) under UV light illumination.

The above results shows that CD-Ds were highly selective towards the detection of TCH and DXH.

To check the anti-interference ability of these CD-Ds towards TCH and DXH sensing in the presence of other pharmaceuticals, we have performed competitive experiment in the presence of 1.0 equivalent of various interference pharmaceuticals and 1.0 equivalent of TCH and DXH pharmaceuticals. Figure 9C displays that our CD-Ds system exhibits good selectivity and anti-interference capability towards TCH and DXH. It means that our sensor detects TCH and DXH even in the presence of other pharmaceuticals. We got almost similar results towards TCH and DXH during the selectivity experiment which shows that other pharmaceuticals do not affects the sensing capability of CD-Ds. Figure 9D clearly evident that there is no change in the blue luminescence of CD-Ds in the presence of other pharmaceuticals. Similarly, the PL spectra of CD-Ds remains constant in the presence of other interfering pharmaceuticals. This photograph indicates the selective changes in the PL intensity of CD-Ds towards TCH and DXH which further collaborates with the fluorescence studies carried out earlier.

3.3. Sensitivity Experiments

We have performed sensitivity experiments of CD-Ds towards TCH and DXH sensing. The PL intensity variation of CD-Ds was proportional to the concentration of TCH and DXH in the range between 1-50 μM, which was described by the Stern-Volmer equation. The Stern-Volmer plots display a good linear relationship (R^2 = 0.9991) with TCH and DXH concentrations in range 1-50 μM with Stern-Volmer constant of 2.3×10^4 M^{-1} (Figure 10A, B).
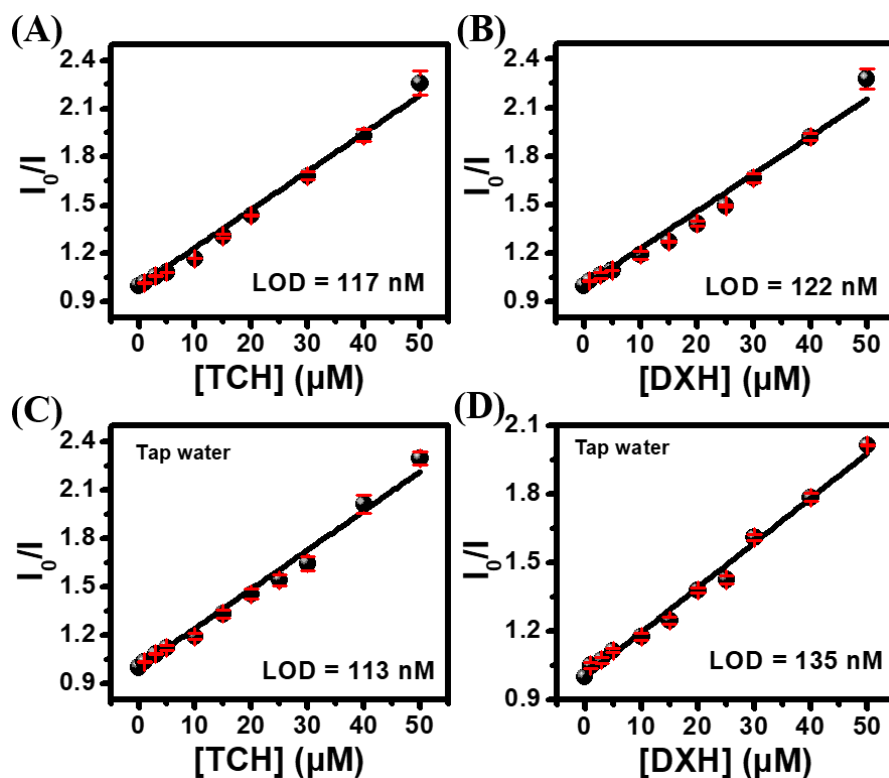
Figure 10. Stern Volmer plots of CD-Ds with TCH and DXH, respectively, concentrations (1-50 μM) in the presence of (A, B) Milli-Q and (C, D) tap water.

These Stern-Volmer (SV) plots exhibit high binding affinity of TCH and DXH towards CD-Ds. The calculated limit of detection (LOD) of TCH and DXH for CD-Ds are 117 and 122 nM, respectively. We have performed similar experiments in tap water also. Our findings reveal that the LOD of TCH and DXH with CD-Ds in tap water, are 113 and 135 nM which show almost similar response as compared to Milli-Q water (Figure 10C, D). It is clearly evident that the calculated LOD of TCH and DXH with CD-Ds, show similar sensitivity and highly selectivity in Milli-Q water as well as tap water.

3.4. Mechanism of TCH and DXH Sensing

We have captured CLSM images to show the luminescence nature of CD-Ds in the absence and presence of TCH and DXH. Figure 11 shows the CLSM images (DIC, fluorescence) of CD-Ds in absence and presence of TCH and DXH.
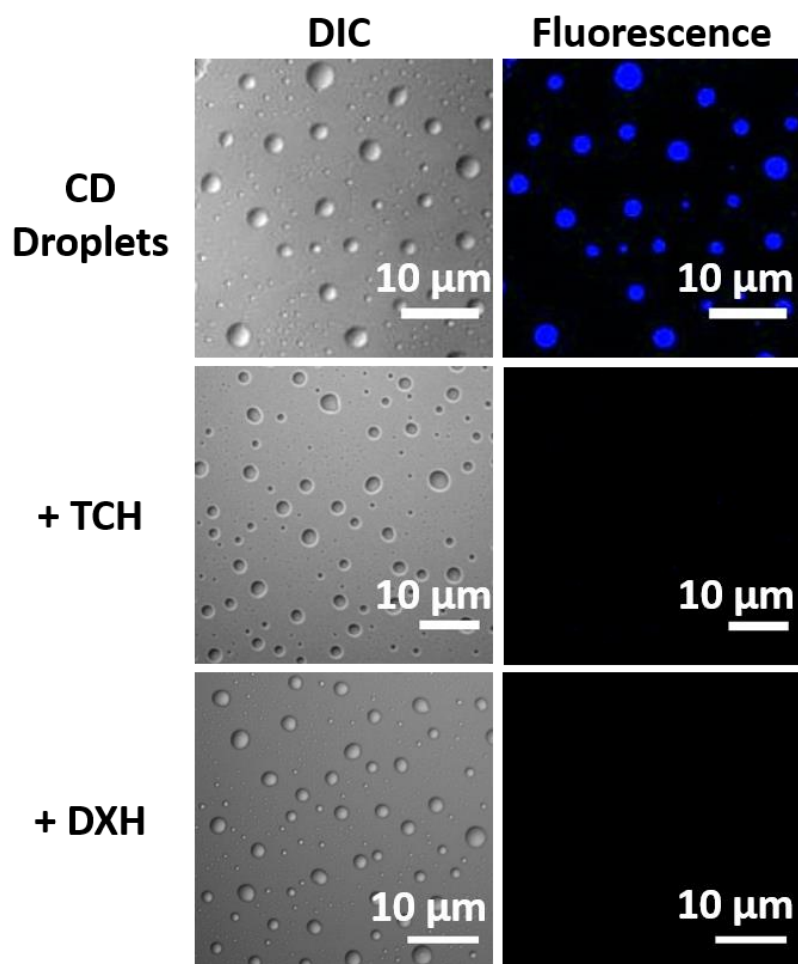
Figure 11. Confocal images (DIC, fluorescence) in the absence and presence of TCH and DXH.

In case of bare CD-Ds, DIC image displays well dispersed stable droplets and fluorescence image shows the blue emissive CDs.[36] This blue emission looks homogeneous throughout these droplets and reveals that

there are blue emissive CDs inside these droplets uniformly distributed. There are CLSM images (DIC, fluorescence) of CD-Ds in the presence of TCH and DXH. Both DIC images show the well spherical stable droplets and homogeneously distributed in the presence of TCH and DXH. But fluorescence images do not display luminescence behavior in the presence of TCH and DXH and the blue emission completely disappeared. It indicates that both TCH and DXH interact with these CD-Ds and quench its PL intensity.

To explore the sensing mechanism and interaction between CD-Ds and pharmaceuticals, we have explored time resolved PL lifetime of CDs and CD-Ds in the presence and absence of TCH and DXH.
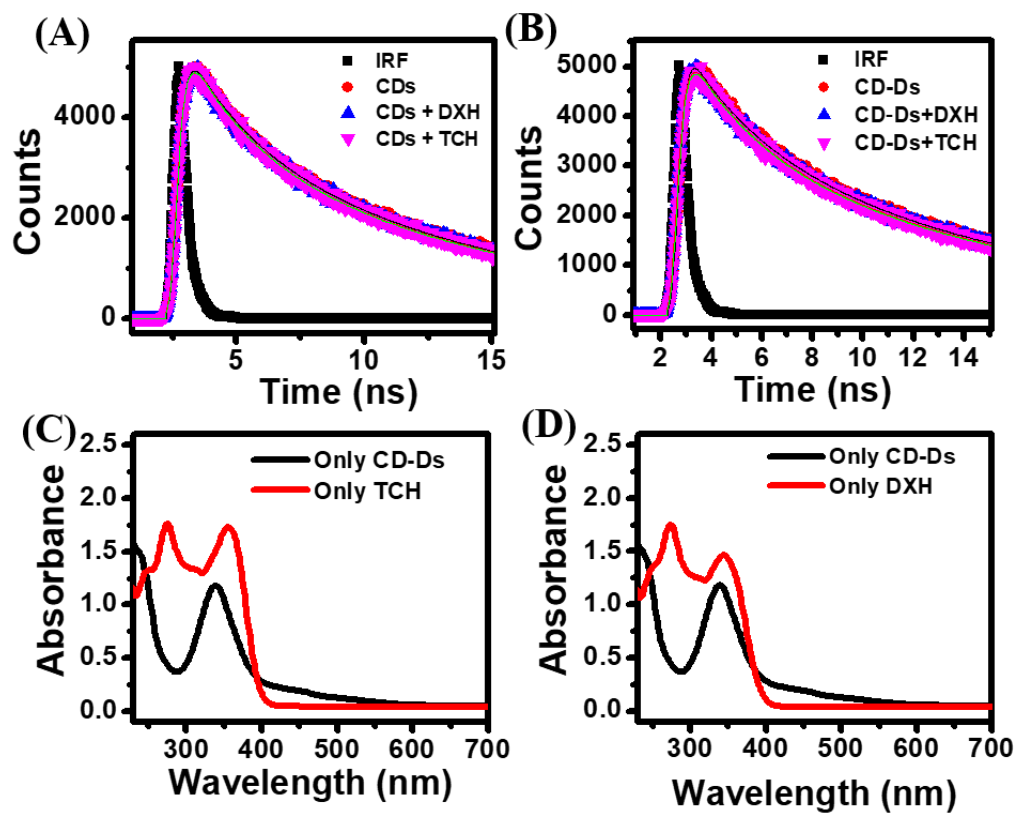
Figure 12. PL decay curves in the absence and presence of TCH and DXH of (A) CDs and (B) CD-Ds. UV spectra of Only CD-Ds and (C) TCH or (D) DXH.

Figure (12A, B) exhibits the PL decay traces (λ_{em}=442 nm; λ_{ex}=334 nm) of CDs and CD-Ds in the presence and absence of 50 μM TCH and DXH. Herein, the PL lifetime of CDs and CD-Ds do not change in the presence of 50 μM TCH and DXH. Therefore, dynamic quenching is not happening in this case.

But Figure (12C, D) shows the absorption spectrum of TCH and DXH. It is clearly visible that the absorption spectra of both TCH and DXH overlap with the excitation spectrum of CDs which is confirmed by using UV-vis spectrophotometer. It is clearly indicating that the mechanism is inner filter effect (IFE) due to the possibility of IFE depends on the extent overlapping in between the excitation or emission spectrum of fluorophore and absorption spectrum of quencher.[39,40] Furthermore, there is no ground state complex formation in this sensing process by which confirms that static quenching is not happening also. Our findings reveal that there is IFE mechanism in this sensing process.

3.5. Photocatalytic Degradation of TCH and DXH

To check another applicability of our present CD-Ds system, we utilized CD-Ds for the photocatalytic degradation of TCH and DXH under blue light illumination. Further, we estimated the partition coefficient K values of TCH/DXH-loaded CD-Ds using UV-vis spectroscopy. The K values were estimated to be 9.4 ± 0.2 and 7.9 ± 0.1, respectively which shows that TCH and DXH are present inside the droplets. Scheme 4 shows the schematic representation in which TCH and DXH are present inside the CD-Ds.

Scheme 4. Schematic Illustration of CD-Ds in Presence of TCH and DXH
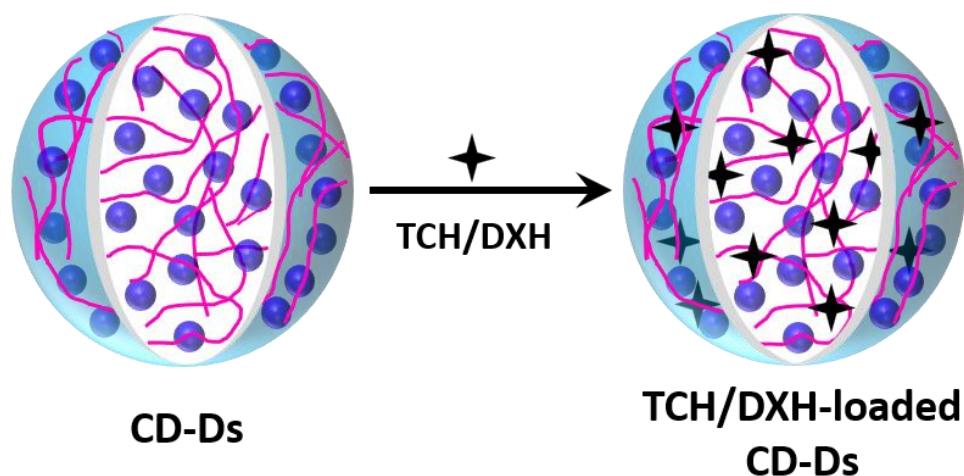
For photocatalytic degradation of TCH and DXH, we utilized a 40 W blue LED (440 nm) for TCH and DXH loaded CD-Ds at room temperature. We have monitored the changes in absorbance spectra and its peak positions in the photocatalytic reaction kinetics by taking UV-vis absorption spectra. Absorption peaks are appeared at 356 and 345 nm of TCH and DXH, respectively. Some control experiments exhibit inappreciable photocatalytic degradation of TCH and DXH in the presence of pH 7.4 aqueous medium of constant blue light irradiation for 75 min. Further, we have explored similar experiment in the presence of ATP-NDs but there is no such degradation in it due to absence of any catalytic unit inside these ATP-NDs. Therefore, there is a need of good photocatalyst for degradation of TCH and DXH.

Afterwards, we have taken CDs and CD-Ds as photocatalyst for TCH and DXH degradation under blue light illumination for 75 min. We have observed the % degradation of TCH and DXH in the presence of bare CDs and CD-Ds as we can see in kinetic plots (Figure 13).
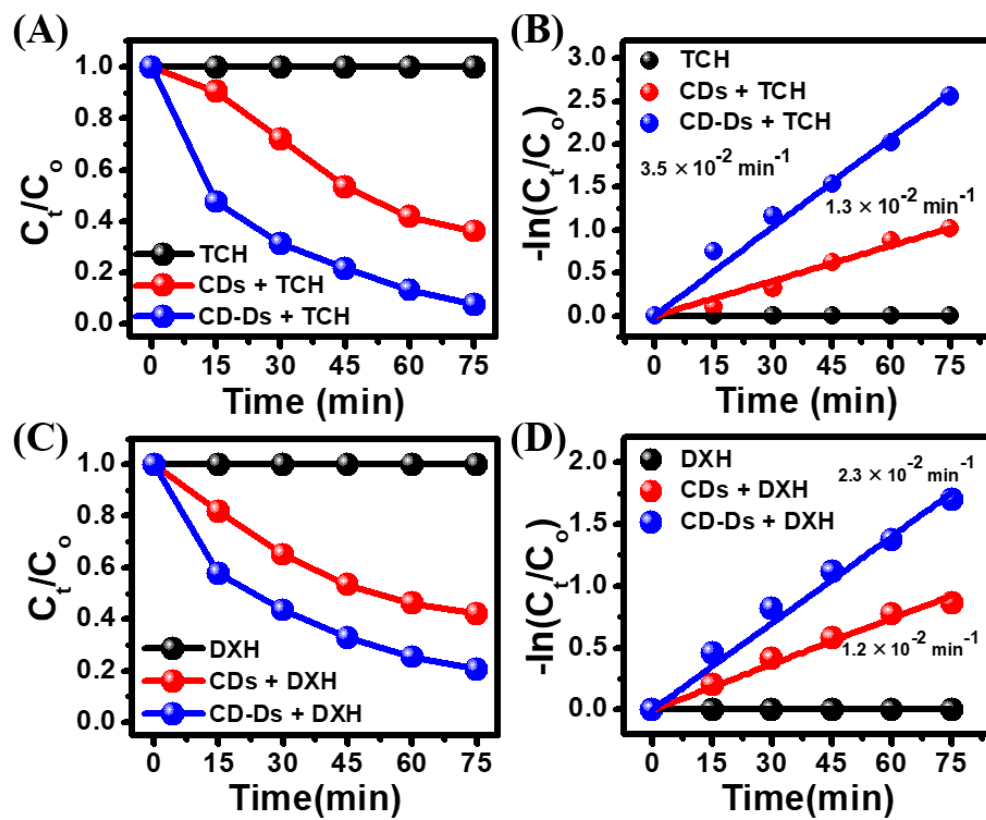
Figure 13. C_t/C_o plots of (A) TCH and (C) DXH at different conditions under blue light illumination for 75 min. The first order kinetics plots of -ln(C_t/C_o) *vs* time for (B) TCH and (D) DXH at different conditions under blue light illumination for 75 min.

These observations suggest that there are almost 92% and 80% degradation of TCH and DXH with CD-Ds, respectively, under blue light illumination for 75 min (Figure 13A, C). Our present CD-Ds system is also good for TCH and DXH degradation in the presence of sunlight. Almost 80% degradation for TCH and DXH, is observed in the presence of sunlight for 75 min. We have fitted our experimental data by using first order kinetic equation and found the rate constant values for bare CDs and CD-Ds from the slopes of these kinetic plots. Figure 13B shows the rate constant value for TCH degradation in presence of CD-Ds, is 3.5×10^{-2} min^{-1} which is 2.7 times higher than in case of bare CDs (1.3×10^{-2} min^{-1}).

Figure 13D shows the rate constant value for DXH degradation, is 2.3×10^{-2} min^{-1} in the presence of CD-Ds which is 1.9 times higher than that in the presence of bare CDs (1.2×10^{-2} min^{-1}). Our observations suggest that this prominent enhancement of TCH and DXH degradation with CD-Ds as compared to bare CDs under blue light irradiation, can be happen because these TCH and DXH are present near the surface of CDs which are embedded inside these droplets. That's why our present CD-Ds system is good photocatalyst for the photocatalytic degradation of TCH and DXH.

3.6. Possible Reaction Mechanism

To find the active species of radicals, we have explored the radical scavenger test in the TCH and DXH degradation processes like previously reported method[41] (Figure 14A). We have performed some experiments for the photocatalytic degradation of TCH with CD-Ds in the presence of several radical scavengers TBA, EDTA, BQ, N$_2$ atmosphere which are responsible for scavenging ·OH radical, hole (h$^+$) and superoxide (·O$_2^-$) radicals, respectively. There is only 29% degradation of TCH with CD-Ds under blue light illumination in the presence of superoxide radical scavengers; BQ and N$_2$ atmosphere that signifies the major role of superoxide radicals in this photocatalytic degradation process. In the presence of hole scavenger EDTA, there is 59.83% degradation of TCH which confirms the role of holes (h$^+$) also in this photocatalytic degradation process. 91.6% degradation of TCH in the presence of ·OH radical scavenger TBA shows that ·OH radicals does not play any role in this photocatalytic degradation process. These findings reveal that superoxide (·O$_2^-$) and (h$^+$) holes are play a dominant part in the photocatalytic TCH degradation.
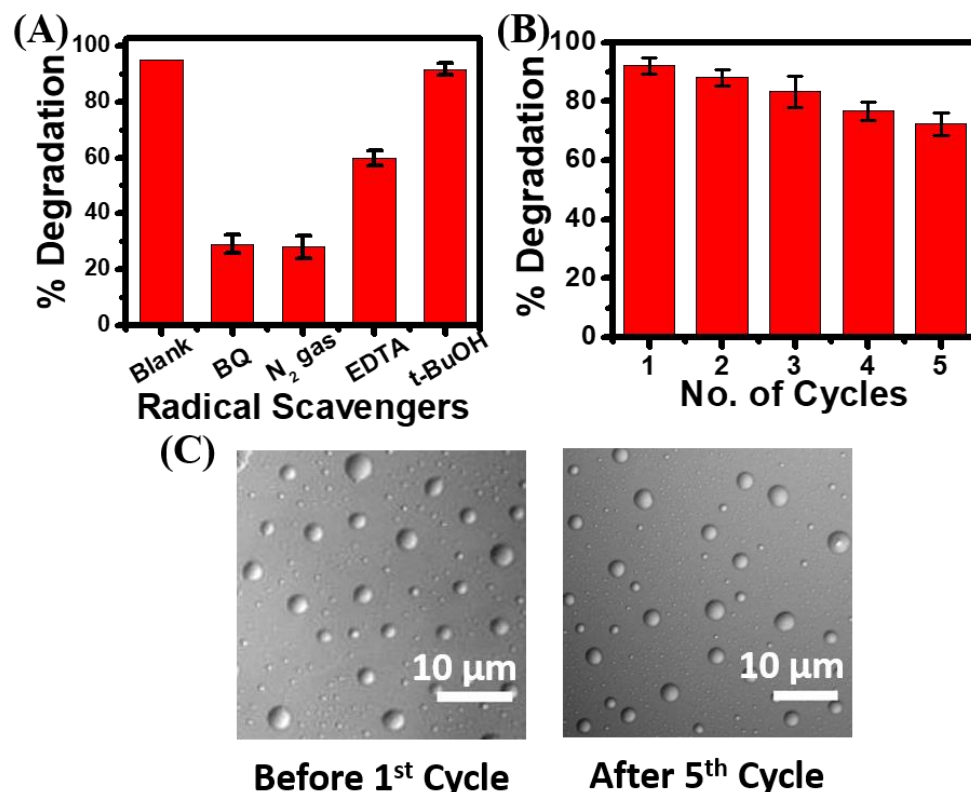
Figure 14. (A) % Degradation of TCH with CD-Ds in the presence of various radical scavengers. (B) Recyclability experiment of CD-Ds for photocatalytic degradation of TCH under blue light illumination for five consecutive runs. Confocal images (DIC) of droplets (C) before first cycle (D) after fifth cycle.

To check the recyclability of our present CD-Ds system, we have explored the recyclability test. We have performed the photocatalytic degradation of TCH inside these CD-Ds for five consecutive cycles (Figure 14B). After each photocatalytic degradation process, these droplets were washed with the help of ethyl acetate to discard byproducts of TCH or unreacted TCH. We have performed similar process 3-4 times for completing our five cycles. There is still >72% degradation inside these CD-Ds under blue light illumination till 5th cycle. Also, we can see in Figure 14C of DIC images of CD-Ds of first cycle and fifth cycle which reveal that there are no prominent structural changes in these CD-Ds. Our

findings reveal that our present CD-Ds system exhibits good recyclability for five consecutive runs without changing its structures.

After seeing the results, we introduced a possible schematic diagram for the photocatalytic TCH degradation under blue light illumination inside the CD-Ds (Figure 15). When the blue light illuminates upon the CDs inside the droplets, it starts to become $e^- \text{—} h^+$ pair (exciton). Atmospheric oxygen gas (O_2) takes the e^-, present in the conduction band of CDs, turns into superoxide radical ($^-O_2$) and these pharmaceuticals changes into byproducts. Holes directly oxidized these pharmaceuticals and breakdown into small products. By using these radicals, TCH and DXH change into small byproducts. Therefore, superoxide radicals and holes (h^+) are responsible for the photocatalytic degradation of TCH and DXH with CD-Ds under blue light illumination.
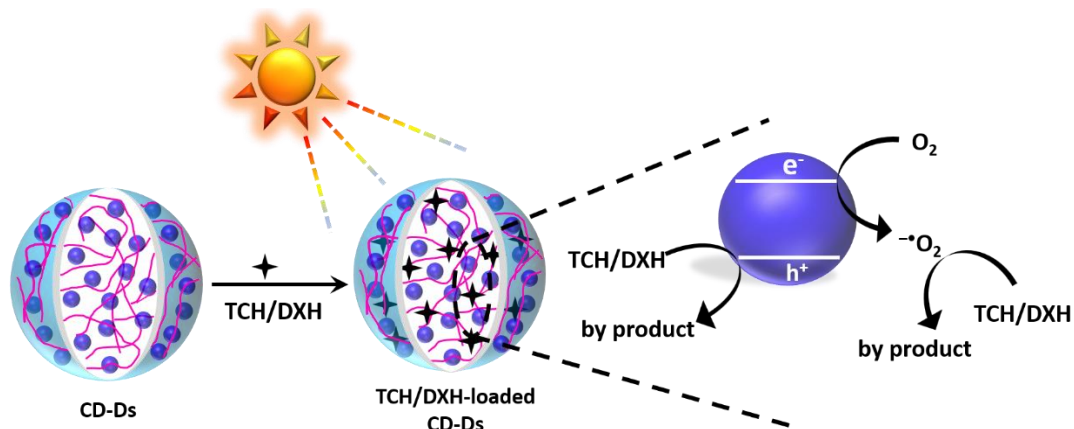
Figure 15. Possible mechanism of photocatalytic degradation of TCH and DXH.

Chapter 4: CONCLUSION AND FUTURE PLAN

Conclusion

We have successfully synthesized CD-Ds and characterized by using various kinds of spectroscopic and microscopic techniques. We have fabricated the CD-Ds utilizing the electrostatic interactions between the anionic CDs and cationic polymer (PDADMAC). Their successful fabrication, shape, structure and morphology were confirmed using different type of spectroscopic and microscopic techniques. Further, we have utilized CD-Ds as a biosensor to detect pharmaceutical contaminants in contaminated water and also used as a photocatalyst to degrade TCH and DXH in the presence of visible light. Our findings reveal that our present CD-Ds system can easily detect as well as degrade TCH and DXH into small byproducts in a fast and economical way. Herein, we observed over 92% and 80% photocatalytic degradation of TCH and DXH inside CD-Ds under visible light illumination for 75 min. Furthermore, superoxide radicals and holes were found to be responsible for the photocatalytic degradation of TCH and DXH. Moreover, our present system shows good recyclability for five consecutive cycles with similar activity. Taken together, our findings clearly reveals that the present CD-Ds are highly stable, and robust in nature. They are further very suitable to be utilized as biosensor as well as photocatalytic nanoreactor for sensing and removal of pharmaceuticals from the contaminated water.

Future Plan

This present work highlights detection as well as degradation of tetracycline hydrochloride and doxycycline hyclate pharmaceuticals with proposed mechanisms. This kind of work can further be extended for the detection and degradation of various other environmental contaminants by fabrication of new different nanoparticle-embedded droplets. Furthermore,

our system can be further utilized to fabricate a water filtration system to purify contaminated water from various pollutants.

Chapter 5:   REFERENCES

(1) Glotzer, S. Nanoscience *vs* Nanotechnology-Defining the Field. *ACS Nano*. **2015,** *9*, 2215-2217.

(2) Bayda, S.; Adeel, M.; Tuccinardi, T.; Cordani, M.; Rizzolio, F. The History of Nanoscience and Nanotechnology: From Chemical-Physical Applications to Nanomedicine. *Molecules* **2020,** *25*, 112.

(3) Esteves da Silva, J.C.G.; Goncalves, H.M.R. Analytical and Bioanalytical Application of Carbon Dots. *TrAC, Trends Anal. Chem.* **2011,** *30*, 1327-1336.

(4) Yang, S.-T.; Cao, L.; Luo, P.G.; Lu, F.; Wang, X.; Wang, H.; Meziani, M.J.; Liu, Y.; Qi, G.; Sun, Y.-P. Carbon Dots for Optical Imaging in Vivo. *J. Am. Chem. Soc*. **2009,** *131*, 11308-11309.

(5) Yang, S.-T.; Wang, X.; Wang, H.; Lu, F.; Luo, P.G.; Cao, L.; Meziani, M.J.; Liu, J.-H.; Liu, Y.; Chen, M. Carbon Dots as Nontoxic and High-Performance Fluorescence Imaging Agents. *J. Phys. Chem. C* **2009,** *113*, 18110-18114.

(6) Cao, L.; Wang, X.; Meziani, M.J.; Lu, F.; Wang, H.; Luo, P.G.; Lin, Y.; Harruff, B.A.; Veca, L.M.; Murray, D. Carbon Dots for Multiphoton Bioimaging. *J. Am. Chem. Soc*. **2007,** *129*, 11318-11319.

(7) Li, Q.; Ohulchanskyy, T.Y.; Liu, R.; Koynov, K.; Wu, D.; Best, A.; Kumar, R.; Bonoiu, A.; Prasad, P.N. Photoluminescent Carbon Dots as Biocompatible Nanoprobes for Targeting Cancer Cells in Vitro. *J. Phys. Chem. C* **2010,** *114*, 12062–12068.

(8) Bayda, S.; Hadla, M.; Palazzolo, S.; Kumar, V.; Caligiuri, I.; Ambrosi, E.; Pontoglio, E.; Agostini, M.; Tuccinardi, T.; Benedetti, A. Bottom-up synthesis of Carbon Nanoparticles with Higher Doxorubicin Efficacy. *J. Control. Release* **2017,** *248*, 144–152.

(9) Vert, M.; Doi, Y.; Hellwich, K.H.; Hess, M.; Hodge, P.; Kubisa, P.; Rinaudo, M.; Schue, F. Terminology for Biorelated Polymers and Applications. *Pure Appl. Chem.* **2012,** *84*, 377-410.

(10) Ekimov, A.I.; Efros, Al.L.; Onushchenko, A.A. Quantum Size Effect in Semiconductor Microcrystals. *Solid State Commun.* **1985,** *56*, 921-924.

(11) Ramirez, H.Y.; Lin, C.H.; Chao, C.C.; Hsu, Y.; You, W.T.; Huang, S.Y.; Chen, Y.T.; Tseng, H.C.; Chang, W.H.; Lin, S.D.; Cheng, S.J. Optical Fine Structures of Highly Quantized InGaAs/GaAs Self-Assembled Quantum Dots. *Phys. Rev. B Condens. Matter* **2010,** *81*, 245324.

(12) Ashoori, R.C. Electrons in Artificial Atoms. *Nature* **1996,** *379*, 413-419.

(13) Murray, C.B.; Kagan, C.R.; Bawendi, M.G. Synthesis and Characterization of Monodisperse Nanocrystals and Close-Packed Nanocrystal Assemblies. *Annu. Rev. Mater. Res.* **2000,** *30*, 545-610.

(14) Senellart, P.; Solomon, G.; White, A. High-Performance Semiconductor Quantum-Dot Single-Photon Sources. *Nat. Nanotechnol.* **2017,** *12*, 218.

(15) Ramasamy, P.; Kim, N.; Kang, Y.S.; Ramirez, O.; Lee, J.S. Tunable, Bright, and Narrow-Band Luminescence from Colloidal Indium Phosphide Quantum Dots. *Chem. Mater.* **2017,** *29*, 6893-6899.

(16) Konstantatos, G.; Sargent, E.H. Nanostructured Materials for Photon Detection. *Nat. Nanotechnol.* **2010,** *5*, 391-400.

(17) Amelia, M.; Lincheneau, C.; Silvi, S.; Credi, A. Electrochemical Properties of CdSe and CdTe Quantum Dots. *Chem. Soc. Rev.* **2012,** *41*, 5728-5743.

(18) Xu, X.; Ray, R.; Gu, Y.; Ploehn, H.J.; Gearheart, L.; Raker, K.; Scrivens. Electrophoretic Analysis and Purification of Fluorescent Single-Walled Carbon Nanotube Fragments. *J. Am. Chem. Soc*. **2004,** *126*, 12736-12737.

(19) Zhu, S.; Meng, Q.; Wang, L.; Zhang, J.; Song, Y.; Jin, H.; Zhang, K.; Sun, H.; Wang, H.; Yang, B. Highly Photoluminescent Carbon Dots for Multicolor Patterning, Sensors, and Bioimaging. *Angew. Chem. Int. Ed.* **2013,** *125*, 4045-4059.

(20) Wang, X.; Cao, L.; Lu, F.; Meziani, M.J.; Li, H.; Qi, G.; Zhou, B.; Harruff, B.A.; Kermarrec, F.; Sun, Y.-P. Photoinduced Electron Transfers with Carbon Dots. *Chem. Commun*. **2009,** *25*, 3774–3776.

(21) Li, Y.; Hu, Y.; Zhao, Y.; Shi, G.; Deng, L.; Hou, Y.; Qu, L. An Electrochemical Avenue to Green-Luminescent Graphene Quantum Dots as Potential Electron-Acceptors for Photovoltaics. *Adv. Mater*. **2011,** *23*, 776–780.

(22) Zhou, L.; Lin, Y.; Huang, Z.; Ren, J.; Qu, X. Carbon Nanodots as Fluorescence Probes for Rapid, Sensitive, and Label-Free Detection of Hg^{2+} and Biothiols in Complex Matrices. *Chem. Commun.* **2012,** *48*, 1147–1149.

(23) Liu, L.; Li, Y.; Zhan, L.; Liu, Y.; Huang, C. One-step Synthesis of Fluorescent Hydroxyls-Coated Carbon Dots with Hydrothermal Reaction and its Application to Optical Sensing of Metal Ions. *Sci. China Chem*. **2011,** *54*, 1342–1347.

(24) Keating, C.D. Aqueous Phase Separation as a Possible Route Compartmentalization of Biological Molecules. *Acc. Chem. Res.* **2012,** *45*, 2114-2124.

(25) Shin, Y.; Brangwynne, C. P. Liquid Phase Condensation in Cell Physiology and Disease. Science 2017, 357 (6357).

(26) Boeynaems, S.; Alberti, S.; Fawzi, N. L.; Mittag, T.; Polymenidou, M.; Rousseau, F.; Schymkowitz, J.; Shorter, J.; Wolozin, B.; Van Den Bosch, L.; Tompa, P.; Fuxreiter, M. Protein Phase Separation: A New Phase in Cell Biology. *Trends Cell Biol.* **2018,** *28* (6), 420-435.

(27) Banani, S.F.; Lee, H.O.; Hyman, A.A.; Rosen, M.K. Biomolecular Condensates: Organizers of Cellular Biochemistry. *Nat. Rev. Mol. Cell Biol.* **2017,** *18* (5), 285-298.

(28) Welsh, T.J.; Krainer, G.; Espinosa, J.R.; Joseph, J.A.; Sridhar, A.; Jahnel, M.; Arter, W.E.; Saar, K.L.; Alberti, S.; Guevara, R.C.; Knowles, T.P.J. Surface Electrostatics Govern the Emulsion Stability of Biomolecular Condensates. *Nano Letters* **2022**, *22* (2), 612-621.

(29) Li, P.; Zeng, X.; Li, S.; Xiang, X.; Chen, P.; Li, Y.; Liu, B.F. Rapid Determination of Phase Diagrams for Biomolecular Liquid–Liquid Phase Separation with Microfluidics. *Analytical Chemistry* **2022**, *94* (2), 687-694.

(30) Liu, G.N.; Xu, R.D.; Zhao, R.Y.; Sun, Y.; Bo, Q.B.; Duan, Z.Y.; Li, Y.H.; Wang, Y.Y.; Wu, Q.; Li, C. Hybrid Copper Iodide Cluster-Based Pellet Sensor for Highly Selective Optical Detection of *o*-Nitrophenol and Tetracycline Hydrochloride in Aqueous Solution. *ACS Sustain. Chem. Eng.* **2019,** *7*, 18863-18873.

(31) Vaishnav, J.K.; Mukherjee, T.K. Long-Range Response Coupling-Induced Surface Energy Transfer from CdTe Quantum Dot to Plasmonic Nanoparticle. *J. Phys. Chem. C* **2018,** *122*, 28324-28336.

(32) Vaishnav, J.K.; Mukherjee, T.K. Surfactant-Induced Self Assembly of CdTe Quantum Dots into Multicolor Luminescent Hybrid Vesicles. *Langmuir* **2019,** *35*, 6409−6420.

(33) Bhattacharya, A.; Chatterjee, S.; Prajapati, R.; Mukherjee, T.K. Size-Dependent Penetration of Carbon Dots inside the Ferritin Nanocages:

Evidence for Quantum Confinement Effect in Carbon Dots. *Phys. Chem. Chem. Phys.* **2015,** *17*, 12833-12840.

(34) Bhattacharya, A.; Chatterjee, S.; Khorwal, V.; Mukherjee, T.K. Luminescence Turn-on/off Sensing of Biological Iron by Carbon Dots in Transferrin. *Phys. Chem. Chem. Phys.* **2015,** *18*, 5148-5158.

(35) Singh, S.; Vaishnav, J.K.; Mukherjee, T.K. Quantum Dot-Based Hybrid Coacervate Nanodroplets for Ultrasensitive Detection of Hg^{2+}. *ACS Appl. Nano Mater.* **2020,** *3*, 3604-3612.

(36) Saini, B.; Singh, R.R.; Nayak, D.; Mukherjee, T.K. Biocompatible pH-Responsive Luminescent Coacervate Nanodroplets from Carbon Dots and Poly(diallyldimethylammonium chloride) Toward Theranostic Applications. *ACS Appl. Nano Mater.* **2020,** *3*, 5826-5837.

(37) Chatterjee, S.; Mukherjee, T.K. Size-Dependent Differential Interaction of Allylamine-Capped Silicon Quantum Dots with Surfactant Assemblies Studied using Photoluminescence Spectroscopy and Imaging Technique. *J. Phys. Chem. C* **2013,** *117*, 10799−10808.

(38) Karakocak, B.B.; Liang, J.; Kavadiya, S.; Berezin, M.Y.; Biswas, P.; Ravi, N. Optimizing the Synthesis of Red-Emissive Nitrogen Doped Carbon Dots for Use in Bioimaging. *ACS Appl. Nano Mater.* **2018,** *1*, 3682−3692.

(39) Shang, L.; Dong, S. Design of Fluorescent Assays for Cyanide and Hydrogen Peroxide Based on the Inner Filter Effect of Metal Nanoparticles. *Anal. Chem.* **2009,** *81*, 1465-1470.

(40) Zheng, M.; Xie, Z.; Qu, D.; Li, D.; Du, P.; Jing, X.; Sun, Z. On-Off-On Fluorescent Carbon Dot Nanosensor for Recognition of Chromium(VI) and Ascorbic Acid Based on the Inner Filter Effect. *ACS Appl. Mater. Interfaces* **2013,** *5*, 13242-13247.

(41) Singh, S.; Rao, C.; Nandi, C.K.; Mukherjee, T.K. Quantum Dot-Embedded Hybrid Photocatalytic Nanoreactors for Visible Light Photocatalysis and Dye Degradation. *ACS Appl. Nano Mater*. **2022,** *5*, 7427-7439.